Spatiotemporal optical bullets in two-dimensional fiber arrays and their stability

Alejandro B. Aceves,[1] Olga V. Shtyrina,[2,3] Alexander M. Rubenchik,[4] Mikhail P. Fedoruk,[2,3] and Sergei K. Turitsyn[2,5]
[1]*Department of Mathematics, Southern Methodist University, Dallas, Texas 75275, USA*
[2]*Novosibirsk State University, Novosibirsk, Pirogova 2, 630090, Russia*
[3]*Institute of Computational Technologies, Novosibirsk, Lavrentjeva 6, 630090, Russia*
[4]*Lawrence Livermore National Laboratory, Livermore, California 94550, USA*
[5]*Aston Institute of Photonic Technologies, Aston University, Birmingham, B4 7ET, United Kingdom*
(Received 28 October 2014; published 11 March 2015)

Long-lived light bullets fully localized in both space and time can be generated in novel photonic media such as multicore optical fiber or waveguide arrays. In this paper we present detailed theoretical analysis on the existence and stability of the discrete-continuous light bullets using a very generic model that occurs in a number of applications.

DOI: 10.1103/PhysRevA.91.033810 PACS number(s): 42.65.Tg, 05.45.Yv, 42.65.Re, 42.81.Qb

Structuring of light in space and time is a fascinating area of research and technology. In space, light can be localized and structured by using waveguides that are formed by appropriate variations of the refractive index. Nonlinear optics gives another practical possibility to localize and control light, both in space and time. The combination of these two features leads to a rich variety of interconnected methods to structure and manipulate spatial and temporal properties of light. In particular, advances in fiber-optics technology over the past 30 years [1,2], has had an impact not only in numerous highly important applications, but it has also provided a laboratory to display nonlinear phenomena such as modulation instability, solitons formation and interactions, supercontinuum generation, parametric amplification, optical wave turbulence, and many others. In space, even earlier, the possibility of balancing diffraction with nonlinear self-focusing so that localized wave packets could propagate undistorted emerged as an important topic with broad applicability.

The theory of soliton formation and its instability in the 1+2 dimensional nonlinear Schrödinger equation (NLSE), $i\partial_z U(x,y,z) + \Delta_T U + \gamma|U|^{2\sigma}U = 0$, proved that for the focusing Kerr nonlinearity (γ positive and $w$log equal to 1) and $\sigma = 1$, a $2d$ spatial soliton is unstable in that it either collapses (for powers above critical) or diffracts. In this equation, u represents the envelope of the electric field; T stands for the spatial variables (x,y) that are transverse to the direction of propagation z. At the so-called critical case ($\sigma d = 2$, $d =$ transverse dimension), collapse is arrested by various additional terms in the model even if they are small. Most common examples are nonlinear losses and nonlinearity saturation. In bulk media, localization both in space and time through collapse under the combined effect of diffraction, anomalous dispersion, and nonlinear refraction leads to formation of small-scale spatiotemporal optical structures pulses, or light bullets [3].

A mechanism of practical importance for wave collapse stabilization and the formation of localized solutions (light bullets) is the system discreteness. In particular, if instead of a continuum field we have a discrete model with the corresponding discrete Laplacian, our earlier pioneering work [4,5] demonstrated in a specific rectangular geometry of waveguide arrays that stable bullets propagate in such a model. As it has been the case in other instances, it was years later that this theoretical discovery was demonstrated experimentally. At the time, we witnessed technological advances in photonic crystals and multicore fibers. Driven by major challenges in optical communication to provide methods and techniques capable of offering transmission capacity above the limitations of the single-mode-fiber communication channel [6–8], the multicore fiber (MCF) allows one to implement spatial division multiplexing, enabling a scale up in transmission capacity per fiber. Recent experimental demonstration of light bullets (LBs) in an array of optical waveguides [9,10] paves the way for broad applications of light bullets in relatively low cost MCFs. As the technology of multicore fibers continues to advance, so are the possible applications of such arrays. Note that spatial demultiplexing is also important in emerging applications of multicore fibers in high-power fiber lasers [11,12].

Here, the use of multicore fiber allows one to split the total high power into channels with power below any undesirable nonlinear effects. In other words, laser beams in each core may be transported safely, being below the threshold of the detrimental nonlinear effects while the total coherently combined power can be high. In this respect, our work represents an important contribution to this application in that it studies the stability properties of LB under more general coupling schemes. Finally, this multicore fiber technology opens up new perspectives for fascinating research on light bullets (see, e.g., [13–22] and references therein) and can be a natural laboratory to study fundamental phenomena such as nonlinear Anderson localization [14], optical rogue wave formation [15], slow light bullets [16], and applications such as delivery of high-power and high-energy light [17,18], to name some. The MCF is a specific realization of fiber arrays with flexible mutual arrangement of cores. It is important to understand how the mutual arrangement of fibers will affect the existence of LBs and their stability, which is the subject of the present work.

In this paper we present a thorough analytical description of localized bullets and complete analysis of their stability. The numerical calculations support the analytical results and demonstrate the range of applicability of the analytical approach. Finally, we demonstrate the formation of the stable light bullet from the a pulse launched in one fiber core. Given the importance of LBs in nonlinear science and the applications mentioned above and a variety of possible implementations of

MCFs, the main objective of this work is to analyze the optical bullet features in continuous-discrete optical media, including their stability under the most general coupling schemes. Our focus is on the generic models that may be applied in various applications. This theoretical work we believe will provide a framework in the design of multicore elements aimed at optimizing desirable and specific applications such as routing, switching, and coherent beam combination.

For arrays of waveguides where light propagates mainly in the central (core) region of the individual elements and for which transverse exchange of energy is due to tails of the field overlapping neighbor waveguides, the field is well approximated by a superposition

$$E(x,y,z,t) = \sum_{nm} U_{nm}(z)F(x-x_m, y-y_m)e^{i(kz-\omega t)} + \text{c.c.},$$

where we assume each waveguide is identical and supports a single mode F. The center of each waveguide is at location (x_m, y_m). In this case the equations, in the weak-coupling approximation, describing the propagation of the envelopes propagating in the fiber at site (n,m) read

$$i\partial_z U_{nm} + (\underline{\underline{C}}\,\underline{U})_{n,m} + \frac{\beta_2^{nm}}{2}\partial_t^2 U_{nm} + 2\gamma_{nm}|U_{nm}|^2 U_{nm} = 0, \tag{1}$$

where $(\underline{\underline{C}}\,\underline{U})_{nm}$ represents the linear coupling functional form at site (n,m), $\beta_2^{nm}(k)$ is the group velocity dispersion, and γ_{nm} the Kerr parameter of each individual core. Here we assume the cores to be identical, thus $\beta_2^{nm} = \beta_2, \gamma_{nm} = \gamma$. Introducing dimensionless variables by the transformations $cz \to z, tT \to t, \sqrt{\frac{\gamma}{c}}U \to U; T = \sqrt{\frac{\beta_2}{2c}}$ leads to the dimensionless equation to be studied in the rest of the paper:

$$i\partial_z U_{nm} + \left(\frac{1}{c}\underline{\underline{C}}\,\underline{U}\right)_{n,m} + \partial_t^2 U_{nm} + |U_{nm}|^2 U_{nm} = 0. \tag{2}$$

We should point out that the effective nonlinearity depends not only on material nonlinearity but on the coupling coefficient, which can be changed by variations in the distance between the cores. The amplitude of the radiation in the cores is limited by the variety of the nonlinear effects (SBS, SRS, optical damage). The coupling dependence of the effective nonlinearity gives a possibility always to find regimes where our results will be applicable by a suitable change in the effective coefficient. To emphasize how the specific scalings differ from application to application, consider, for example, the recent work in [23] which considers self-focusing for fibers with six or seven cores, each of 6 μm diameter, 15 μm core-to-core distance, a nonlinear index of refraction of $n_2 = 2.2 \times 10^{-20}$ m^2/W, a signal at a wavelength of 1064 nm, and the simulations extend to 8 cm. If instead the application of multicore fibers is to build a passive optical network [7], the characteristics of the individual cores, core-to-core separation, propagation distances, powers, and wavelength used are quite differently, yet the physical principles are the same; thus both cases after proper scaling can be modeled to first approximation by the the equation above.

Two cases of interest are (see Fig. 1) the uniform square and the hexagonal geometries, for which the respective coupling

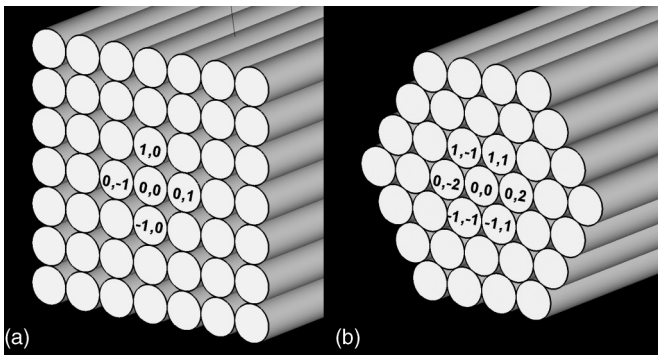

FIG. 1. Square and hexagonal waveguide structures.

operators are as follows:

$$(\underline{\underline{C}}\,\underline{U})_{nm}^{\text{square}} = c(U_{n-1,m} + U_{n+1,m} + U_{n,m-1} + U_{n,m+1})$$

$$(\underline{\underline{C}}\,\underline{U})_{nm}^{\text{hexagon}} = c(U_{n-1,m-1} + U_{n-1,m+1} + U_{n,m-2} + U_{n,m+2} + U_{n+1,m-1} + U_{n+1,m+1}).$$

This system has two known conserved quantities: the Hamiltonian $H = \sum_{nm}\int(N(\underline{U};\underline{U})_{nm} - |\partial_t U_{nm}|^2 + |U_{nm}|^4)dt$ and the total power $P = \sum_{nm}\int |U_{nm}|^2 dt$.

The waveform of the discrete-continuous light bullets (that are extrema of the Hamiltonian under fixed total power P) $U_{nm}(z,t) = A_{nm}(t)e^{i\lambda z}$ is given by the equation

$$-\frac{\delta(H+\lambda P)}{\delta A_{nm}^*} = -\lambda A_{nm} + (\underline{\underline{C}}\,\underline{A})_{nm} + \partial_{t^2}^2 A_{nm} + 2|A_{nm}|^2 A_{nm} = 0.$$

Highly localized bullet solutions in some limits can be derived using an asymptotic approach. The consideration is that spatially most of the energy is concentrated in one site, (0,0), and small satellite pulses of decreasing amplitude propagate in subsequent layers. Mathematically, this means we seek solutions of the form $U_{nm}(z,t) = A_{nm}(t)e^{i\lambda z} +$ c.c. with $\lambda \gg 1$, where each envelope has an expansion of the form $A_{nm}(t) = A_{nm}^{(0)}(t;\lambda) + A_{nm}^{(1)}(t;\lambda) + A_{nm}^{(2)}(t;\lambda) + \cdots$.

The analytical derivation of the asymptotic solutions is straightforward [4] and we only present here the expressions for the central core and the first layer for the square and hexagonal arrays (see corresponding indices and notations below):

$$A_{0,0}^{\text{square}}(t) = a_0(t) + O\left(\frac{1}{\lambda^{5/2}}\right) = \frac{\sqrt{\lambda}}{\cosh(\sqrt{\lambda}t)} + O\left(\frac{1}{\lambda^{5/2}}\right),$$

$$A_{\pm1,0}^{\text{square}}(t) = A_{0,\pm1}^{\text{square}} = a_1(t) + O\left(\frac{1}{\lambda^{5/2}}\right) = \frac{c}{2\sqrt{\lambda}}[e^{\sqrt{\lambda}t}\ln(1+e^{-2\sqrt{\lambda}t}) + e^{-\sqrt{\lambda}t}\ln(1+e^{2\sqrt{\lambda}t})] + O\left(\frac{1}{\lambda^{5/2}}\right),$$

$$A_{0,0}^{\text{hex}}(t) = a_0(t) + O\left(\frac{1}{\lambda^{3/2}}\right),$$

$$A_{0,\pm2}^{\text{hex}}(t) = A_{1,\pm1}^{\text{hex}} = A_{-1,\pm1}^{\text{hex}} = a_1(t) + O\left(\frac{1}{\lambda^{3/2}}\right).$$

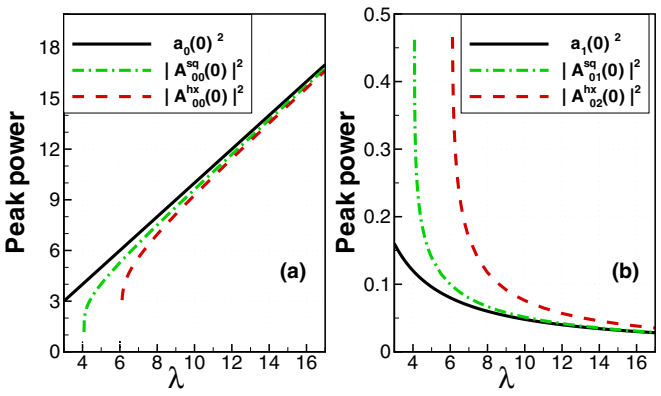

FIG. 2. (Color online) Peak power [numerical (color) and theory (black solid)] vs the parameter λ in central (a) and closer neighbor waveguides (b) for 33×33 square and 33×65 hexagonal waveguide structures.

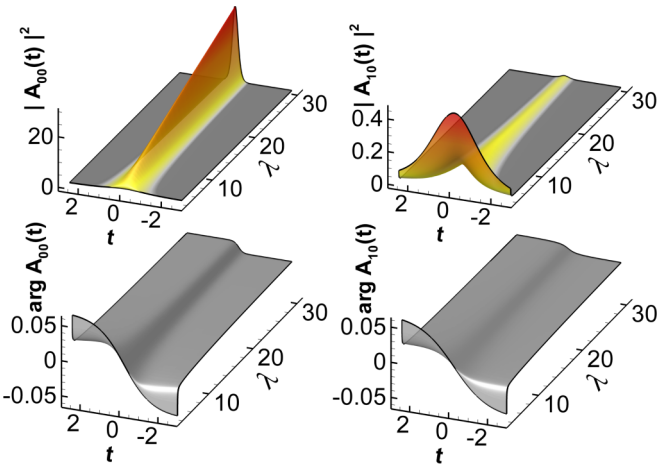

FIG. 4. (Color online) 3D power and phase time distributions vs parameter λ for the central (left) and closer neighbor waveguide (right) for a square waveguide structure.

These solutions, whose leading-order terms a_0, a_1 are obtained in as similar way as in [4], fail to be uniformly valid beyond $|t| \geqslant O(\sqrt{\lambda})$. In fact, at the pulse tails, all waveguides have solutions of the same order $A_{nm} = O(te^{-\sqrt{\lambda}|t|}), t \geqslant \sqrt{\lambda}$. In what follows, we compare these analytical results with numerically computed general localized LB solutions.

Our numerical studies present solutions describing continuous discrete light bullets of Eq. (2), where we varied the number of elements in the array, which is an important consideration for practical systems where the number of cores is finite.

We find that the asymptotic expressions $a_0(t), a_1(t)$ fit the numerically found solutions of the system (3) up to the order $O(\frac{1}{\lambda^{3/2}})$. In Figs. 2 and 3 analytical asymptotic and numerical solutions are compared for $c = 1$ for the rectangular structure with $N \times N$ crossed and the hexagonal structure with $N \times 2N$ crossed. Figure 2 depicts the dependence of the amplitude of the solution in the central and neighboring cores on the parameter λ. Figure 3 shows a comparison of the time-domain structure of the light bullets for two different values of λ. A few observations can be made from Figs. 2 and 3. First, the asymptotic mode fits well with the LBs for large values of $\lambda > 14$ and it is an even better approximation for the square geometry. The second observation is that the theoretical leading-order approximation overshoots the numerical outcome for the central core and underestimates that of the neighbor sites. This can be corrected by computing higher-order terms in more detail, but perhaps more important is that even for values of λ where the approximation is not as good (e.g., $\lambda = 7$), the theoretical approximation represents a good guess for the initial state that will adjust to the LB in propagation. Figure 4 summarizes the spatiotemporal amplitude and phase features of the light bullet, and Fig. 5 shows global characteristics of the LB such as power and the Hamiltonian. We observed that the functional dependence shown here is universal independent of the number of fiber elements (assumed to be large), and is consistent with Fig. 2(a) in [9].

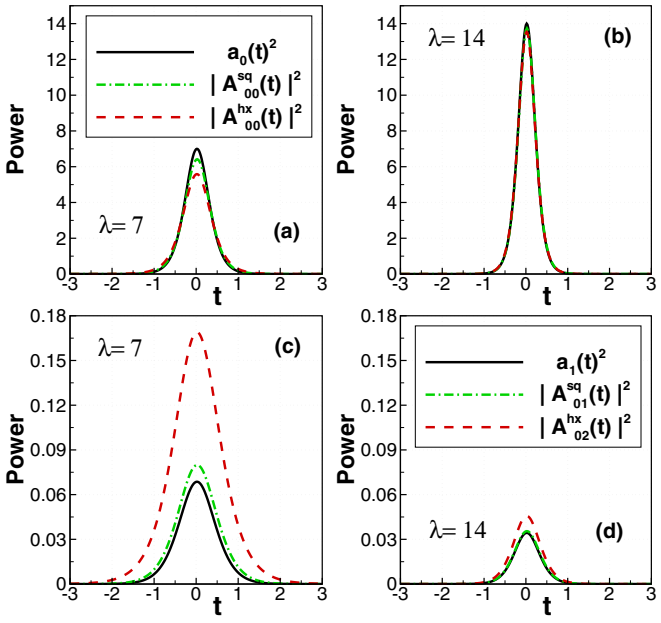

FIG. 3. (Color online) Comparison of numerical solutions (color) with their analytical approximations (black solid) for different λ in the central waveguide (top) and closer neighbor waveguide (bottom) for 33×33 square (green dashed dotted) and 33×65 hexagonal (red dashed) waveguide structures.

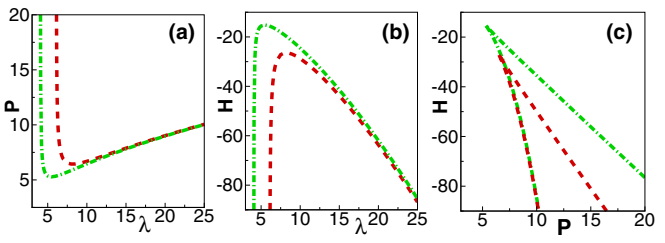

FIG. 5. (Color online) From left to right: (a) dependence of the total power on the parameter λ, (b) dependence of the Hamiltonian on the parameter λ, and (c) the Hamiltonian vs the total power, all for 33×33 square (green dashed dotted) and 33×65 hexagonal (red dashed) waveguide structures.

Next we investigate the stability of solutions of the form $U_{nm}(z,t) = A_{nm}(t)e^{i\lambda z}$ by linearization, $U_{nm}(z,t) = [A_{nm}(t) + f_{nm} + ig_{nm}]e^{i\lambda z}$, leading to the following system of linear equations:

$$-\partial_z g_{nm} = -(\underline{\underline{C}}\,\underline{f})_{nm} - \partial_{t^2}^2 f_{nm} + \lambda f_{nm} - 6|A_{nm}|^2 f_{nm} = (H_- f)_{nm},$$

$$\partial_z f_{nm} = -(\underline{\underline{C}}\,\underline{g})_{nm} - \partial_{t^2}^2 g_{nm} + \lambda f_{nm} - 2|A_{nm}|^2 g_{nm} = (H_+ g)_{nm},$$

or $-\partial_z^2 f_{nm} = [H_+(H_- f)]_{nm}$. We define the inner products for square arrays as follows:

$$\langle \underline{f}, H_+ \underline{f}\rangle = \sum_{nm}\int f_{nm}(H_+ f_{nm})dt = \sum_{nm}\int\left[|A_{nm}|^2\left[\partial_t\left(\frac{f_{nm}}{A_{nm}}\right)\right]^2\right]dt$$

$$+\sum_{nm}\int\left[\left(\sqrt{\frac{A_{n,m-1}}{A_{nm}}}f_{nm} - \sqrt{\frac{A_{n,m}}{A_{n,m-1}}}f_{n,m-1}\right)^2\right]dt + \sum_{nm}\int\left[\left(\sqrt{\frac{A_{n-1,m}}{A_{nm}}}f_{nm} - \sqrt{\frac{A_{n,m}}{A_{n-1,m-}}}f_{n-1,m}\right)^2\right]dt,$$

and for the hexagonal arrays as follows:

$$\langle \underline{f}, H_+ \underline{f}\rangle = \sum_{nm}\int f_{nm}(H_+ f_{nm})dt = \sum_{nm}\int\left\{|A_{nm}|^2\left[\partial_t\left(\frac{f_{nm}}{A_{nm}}\right)\right]^2\right\}dt + \sum_{nm}\int\left[\left(\sqrt{\frac{A_{n,m-1}}{A_{nm}}}f_{nm} - \sqrt{\frac{A_{n,m}}{A_{n,m-1}}}f_{n,m-1}\right)^2\right]dt$$

$$+\sum_{nm}\int\left[\left(\sqrt{\frac{A_{n-1,m}}{A_{nm}}}f_{nm} - \sqrt{\frac{A_{n,m}}{A_{n-1,m-}}}f_{n-1,m}\right)^2\right]dt + \sum_{nm}\int\left[\left(\sqrt{\frac{A_{n+1,m+1}}{A_{nm}}}f_{nm} - \sqrt{\frac{A_{n,m}}{A_{n+1,m+1}}}f_{n+1,m+1}\right)^2\right]dt$$

$$+\sum_{nm}\int\left[\left(\sqrt{\frac{A_{n+1,m-1}}{A_{nm}}}f_{nm} - \sqrt{\frac{A_{n,m}}{A_{n+1,m-1}}}f_{n+1,m-1}\right)^2\right]dt.$$

In both cases and similar to the 1 + 1 + 1 case [24–26], the following properties of the linear operators hold:

(i) $\langle f, H_+ f\rangle \geqslant 0$ and it is equal to 0 if $f_{nm} = 0$ or $f_{nm} = A_{nm}$.

(ii) There exist some $\underline{F}$ for which $\langle -\underline{F}, H_+\underline{F}\rangle$ is negative and $\langle \underline{F}, \underline{A}\rangle = 0$.

We should point out that while we only discussed two specific geometries, (i) and (ii) will be generally true for a large class of coupling schemes. Properties (i) and (ii) allow us to conclude that the existence of negative eigenvalues of the operator H_- is a sufficient condition for instability of the nonlinear state. Furthermore, one can show this condition is equivalent to the Vakhitov-Kolokolov criterion on the sign of $\frac{d}{d\lambda}P = \frac{d}{d\lambda}\langle \underline{A}, \underline{A}\rangle$. Either way, this proves instability of the left branch of solutions in Fig. 5 (left).

For the highly localized solutions of the previous section, one finds that the power $P(\lambda) = 2\lambda^{1/2} + K/\lambda^{3/2}$, where the constant K depends on the coupling coefficient and the geometry, for the square array $K = 5.69$ and for the hexagonal array $K = 8.54$. Observe that a minimum is achieved at $\lambda_c = (3K/2)^{1/2}$, so that stability of the localized ($\lambda > 1$) bullet is assured for coupling strengths below some critical value. This stability criteria is also in agreement with the known stability of one-dimensional solitons, which in this model corresponds to the limit $K \to 0$.

So far, we have demonstrated the existence and stability of the LB localized in several fibers. Now we will demonstrate that the LB can be formed during the propagation of an initial pulse launched from the input faces of the array. Specifically, we simulate the propagation of a Gaussian pulse lunched in one fiber for the hexagonal geometry $U_{0,0}(z = 0,t) = \sqrt{P/(\tau\sqrt{\pi})}\exp[-t^2/(2\tau^2)]$, where $P = 7.48$ in both cases, and $\tau = 0.72$ (a), $\tau = 0.6$ (b).

Figure 6 summarizes the general picture for an incident pulse in a single fiber. The left panel highlights the propagation for $\tau = 0.72$ (smaller input peak power and broader pulse), where according to our analysis, stable LB do not exist. One can observe fast diffraction (in space) and dispersion (in time) of the pulse. The energy in the central core vanishes after $z = 2$, being spread through the surrounding layers. For slightly higher peak power $\tau = 0.6$ (right panel) we observe the formation of LB localized in the center fiber and the surrounding layer. The temporal oscillation can be explained in the following way. The Hamiltonian is conserved in our system and in general, the initial value of H and that of the LB

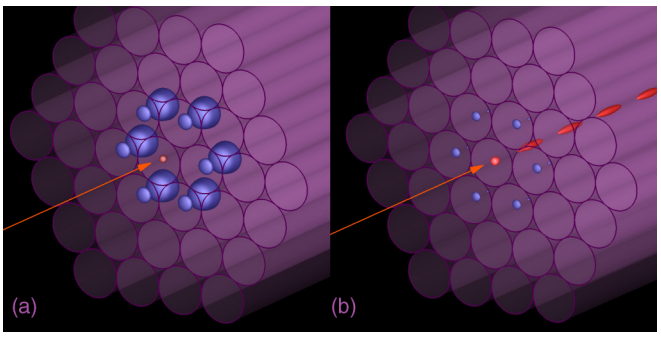

FIG. 6. (Color online) Illustrative depiction of the power spatiotemporal isosurfaces for the propagation of an input Gaussian pulse $U_{0,0}(z = 0,t) = \sqrt{P/(\tau\sqrt{\pi})}\exp[-t^2/(2\tau^2)]$, with $P = 7.48$ and $\tau = 0.72$ (a), $\tau = 0.6$ (b) along the array with the hexagonal geometry. Red isosurfaces of the central core correspond to $|U_{0,0}(z,t)|^2 = 8$ and blue, for the similar power isosurfaces at level 0.16 in the first neighboring cores around the central core. Labeling of core indices as in Fig. 1(b).

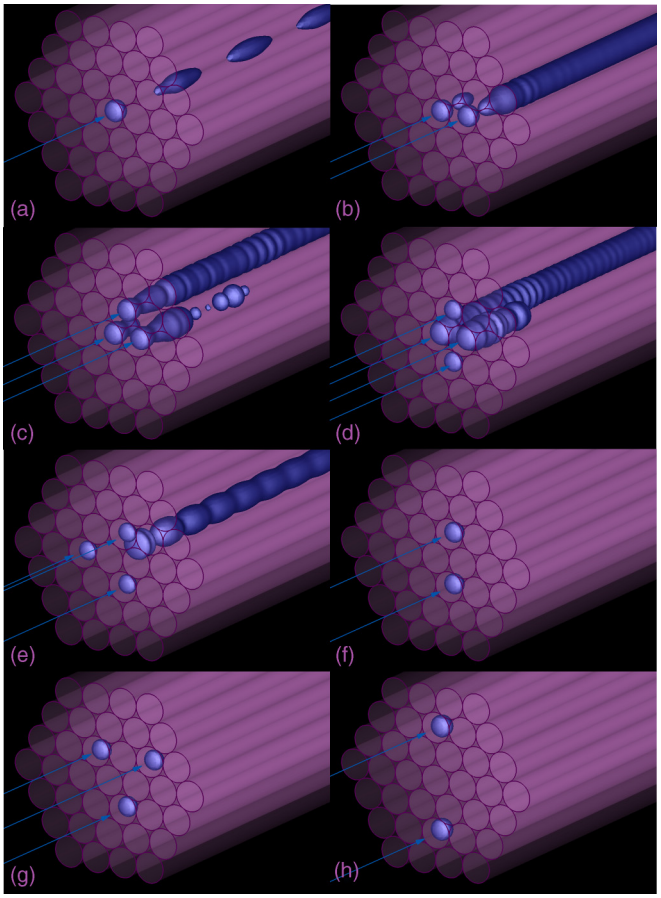

FIG. 7. (Color online) A sample of dynamic scenarios for input pulses in single (a) and multiple (b–h) ports. In (a)–(e) bullets emerge, showing recurrence (a) and symmetry breaking (b–d). Above critical separation between cores and/or below critical power, light propagates in dispersive mode (f–h). Labeling of core indices as in Fig. 1(b).

are different. The adjustment of the Hamiltonian takes place by the radiation in the outside cores carrying out the Hamiltonian difference. Oscillations indicate the residual differences. For reference, red spatiotemporal isosurfaces correspond to the central core, and the blue ones, to the first circle of neighboring cores (with peak power values 50 times less than in the central core). Not shown here is the highly nonlinear regime ($\tau \ll 0.6$) where a localized state propagates in stable fashion. However, one has to consider that at kilowatt power levels, thermal instabilities arise and for short pulses, higher-order linear and nonlinear dispersion effects become relevant and the model has to be adjusted to account for these effects. Finally, Fig. 7 illustrates some of the rich dynamics and fascinating scenarios that can emerge when light propagates in multicore fibers. The figure shows recurrence (a), symmetry breaking (b,c,d), which is also discussed in [13], and transitions from bullet formation (e) to dispersive dynamics (f,g) depending on input power and separation distances when multiple pulses are incident at different cores.

In this work we have studied spatiotemporal light bullet propagation in an optical medium consisting of a multicore fiber or a general array of waveguides, which as this and other recent work indicates, can be used in a variety of applications. We have put forward a comprehensive theoretical framework based on asymptotic and stability analysis that not only validates the existence of stable light bullets, representing light localization in space and time, but it demonstrates they are generic and stable for a multitude of multicore geometries. We also found that they can be formed as a result of the evolution of a sufficiently intense initial pulse launched into the array. We anticipate our results present an opportunity to design array configurations whose topology is suitable for a particular application, including preparing a LB for propagation in bulk Kerr media [27] or in the atmosphere. Our theoretical approach should explain recent work in nonlinear arrays when the model is extended by incorporating higher-order temporal effects [28], or in particular, provide an explanation of the observed additional (large) λ-dependent time shifts, shown in Fig. 7 of Ref. [9]. Clearly such dependence would be quite useful for time delay lines and for efficient coherent pulse combining [29]. The second extension that comes to mind is coupling active fibers, where at first approximation we can add to the model linear gain and saturation. Finally, we concentrated our work to the study of light bullets in the anomalous regime. A natural extension is to perform similar studies to discrete spatiotemporal vortices and other nonlinear modes. With respect to the normal regime, recent experimental results [30] demonstrate the existence of X waves in $1d$ semiconductor waveguide arrays. Theoretically, X waves carry infinite energy, so once a proper renormalization of power and the Hamiltonian is done to the work presented here, an improved existence and stability analysis to $1d$ and $2d$ arrays in the normal dispersion regime can be implemented.

We acknowledge support from a grant from the Ministry of Education and Science of the Russian Federation (Agreement No. 14.B25.31.0003), the Russian Science Foundation (Grant No. 14-21-00110) (the work of O.V.S. and M.P.F.), and the Air Force EOARD (Grant No. FA9550-14-1-0305). This work was partially performed under the auspices of the US Department of Energy by Lawrence Livermore National Laboratory under Contract No. DE-AC52-07NA27344. A.B.A.'s work was supported by the Army Research Department under MURI Grant No. W911NF-11-0297.

[1] P. S. J. Russell, J. Lightwave Technol. **24**, 4729 (2006).
[2] D. J. Richardson, J. Nilsson, and W. A. Clarkson, J. Opt. Soc. Am. B **27**, B63 (2010).
[3] Y. Silberberg, Opt. Lett. **15**, 1282 (1990).
[4] A. B. Aceves, C. DeAngelis, A. M. Rubenchik, and S. K. Turitsyn, Opt. Lett. **19**, 329 (1994).
[5] A. B. Aceves, G. G. Luther, C. DeAngelis, A. M. Rubenchik, and S. K. Turitsyn, Phys. Rev. Lett. **75**, 73 (1995).
[6] F. Y. M. Chan, A. P. T. Lau, and H.-Ya. Tam, Opt. Express **20**, 4548 (2012).
[7] B. Zhu, T. F. Taunay, M. F. Yan, M. Fishteyn, E. Monberg, and F. V. Dimarcello, Opt. Exp. **18**, 11117 (2010).

[8] K. Igarashi, T. Tsuritani, and I. Morita, 1-Exabit/s x km super-Nyquist-WDM multi-core-fiber transmission, ECOC 2014, Mo.3.3.1 (2014).
[9] S. Minardi, F. Eilengerber, Y. K. Kartashov, A. Szameit, U. Röpke, J. Kobele, K. Schuster, H. Bartelt, S. Nolte, L. Torner, F. Lederer, A. Tünnermann, and T. Pertsch, Phys. Rev. Lett. **105**, 263901 (2010); F. W. Wise, Physics **3**, 107 (2010).
[10] F. Eilenberger, S. Minardi, A. Szameit, U. Ropke, J. Kobelke, K. Schuster, H. Bartelt, S. Nolte, L. Torner, F. Lederer, A. Tunnermann, and Th. Pertsch, Phys. Rev. A **84**, 013836 (2011).
[11] B. M. Shalaby, V. Kermene, D. Pagnoux, A. Desfarges-Berthelemot, Barthelemy, A. Popp, M. Abdou Ahmed, A. Voss, and T. Graf, Appl. Phys. B: Lasers Opt. **100** (4), 859 (2010).
[12] H-J. Otto, A. Klenke, C. Jauregui, F. Stutzki, J. Limpert, and A. Tunnermann (unpublished).
[13] F. Eilenberger, S. Minardi, A. Szameit, U. Rnöpke, J. Kobelke, K. Schuster, H. Bartelt, S. Nolte, A. Tnnermann, and Th. Pertsch, Opt. Express **19**, 23171 (2011).
[14] T. Pertsch, U. Peschel, J. Kobelke, K. Schuster, H. Bartelt, S. Nolte, A. Tünnermann, and F. Lederer, Phys. Rev. Lett. **93**, 053901 (2004).
[15] D. R. Solli, C. Ropers, P. Koonath, and B. Jalali, Nature (London) **450**, 1054 (2007).
[16] A. A. Sukhorukov and Y. S. Kivshar, Phys. Rev. Lett. **97**, 233901 (2006).
[17] L. Michaille, C. R. Bennett, D. M. Taylor, and T. J. Shepherd, IEEE J. Sel. Top. Quantum Electron. **15**, 328 (2009).
[18] P. M. Lushnikov and N. Vladimirova, Opt. Lett. **39**, 3429 (2014).
[19] A. B. Blagoeva, S. G. Dinev, A. A. Dreischuh, and A. Naidenov, IEEE J. Sel. Top. Quantum Electron. **27**, 2060 (1991).
[20] D. E. Edmundson and R. H. Enns, Opt. Lett. **17**, 586 (1992); Phys. Rev. A **51**, 2491 (1995).
[21] F. Wise and P. Trapani, Opt. Photonics News **13**, 28 (2002).
[22] B. A. Malomed, D. Mihalache, F. Wise, and L. Torner, J. Opt. B **7**, R53 (2005); L. Torner, S. Carrasco, J. P. Torres, L. C. Crasovan, and D. Mihalache, Opt. Commun. **199**, 277 (2001).
[23] H. Tünnermann, A. Shirakawa, Opt. Express **23**, 2436 (2015).
[24] E. W. Laedke, K. H. Spatschek, and S. K. Turitsyn, Phys. Rev. Lett. **73**, 1055 (1994).
[25] E. W. Laedke, K. H. Spatschek, S. K. Turitsyn, and V. K. Mezentsev, Phys. Rev. E **52**, 5549 (1995).
[26] V. K. Mezentsev, S. L. Musher, I. V. Ryzhenkova, and S. K. Turitsyn, JETP Lett. **60**, 829 (1994).
[27] D. Majus, G. Tamosauskas, I. Grazuleviciute, N. Garejev, A. Lotti, A. Couairon, D. Faccio, and A. Dubietis, Phys. Rev. Lett. **112**, 193901 (2014).
[28] T. X. Tran, D. C. Duong, and F. Biancalana, Phys. Rev. A **90**, 023857 (2014).
[29] M. Kienel, M. Müller, S. Demmler, J. Rothhardt, A. Klenke, T. Eidam, J. Limpert, and A. Tunnermann, Opt. Lett. **39**, 11 (2014).
[30] Y. Lahini, E. Frumker, Y. Silberberg, S. Droulias, K. Hizanidis, R. Morandotti, and D. N. Christodoulides, Phys. Rev. Lett. **98**, 023901 (2007).